Behaviour of heavy metals and natural radionuclides in the mixing of phosphogypsum leachates with seawater

José Luis Guerrero [a,*], Silvia M. Pérez-Moreno [a], Isidoro Gutiérrez-Álvarez [a], , Manuel Jesús Gázquez [b], Juan Pedro Bolívar [a]

[a] Department of Integrated Sciences, Center for Natural Resources, Health and Environment (RENSMA), University of Huelva, 21071, Huelva, Spain. E-mail addresses: joseluis.guerrero@dfa.uhu.es (J.L. Guerrero), silvia.perez@dci.uhu.es (S.M. Pérez-Moreno), isidoro.gutierrez@dfa.uhu.es (I. Gutiérrez), bolivar@uhu.es (J.P. Bolívar).

[b] Department of Applied Physics, University of Cadiz, University Marine Research Institute (INMAR) Cádiz, Spain 11510, Cádiz, Spain. E-mail address: manueljesus.gazquez@uca.es

*Corresponding author. E-mail address: joseluis.guerrero@dfa.uhu.es. Phone number: +34 959 21 9798. Postal address: Department of Integrated Sciences, Center for Natural Resources, Health and Environment (RENSMA), University of Huelva, 21071, Huelva, Spain.

Abstract

Phosphogypsum (PG) is disposed worldwide in large stacks usually placed in coastal zones, as in the case of Huelva (SW of Spain), where around 100 Mt of phosphogypsum are stored on the saltmarshes of the Tinto River estuary covering a surface of about 1000 ha. This management generates the weathering of PG, and due to its high acidity (pH ≈ 2) and pollutant load can provoke significant emissions into their surroundings. In this work were evaluated by laboratory experiments the effects of pH increase in the behaviour of heavy metals and natural radionuclides during the mixing of phosphogypsum leachates with seawater.

The acidic phosphogypsum leachates showed heavy metals concentrations 2-3 orders of magnitude higher than natural continental waters, and natural radionuclides (U-isotopes and ^{210}Po) 4 - 5 orders of magnitude higher than unperturbed aquatic systems. Major elements and some heavy metals as Mn, Ni, Cd, As, Sb and Co showed a conservative behaviour during the neutralization of the leachates with seawater, remaining in the liquid phase, while other ones as Al, Fe, Cr, Zn, Cu, Pb precipitate and/or were adsorbed onto the solid phase. The U-isotopes and ^{210}Po showed a clear non-conservative behaviour probably due to coprecipitation/adsorption processes onto the formed precipitates, but while ^{210}Po reach a total removal at pH ≈ 7, U- isotopes after a total removal at pH ≈ 5, return into the liquid phase due to redissolution/desorption processes at near neutral pH.

The formed precipitates, mainly composed by iron phosphates particles, showed heavy metal and natural radionuclide concentrations from 1 to 3 orders of magnitude higher than unperturbed soils. All these facts demonstrate the serious environmental impact produced by the PG stacks into their surroundings and the urgency of effective restoration measures.

Findings

The main finding is the evaluation of heavy metals and natural radionuclides behaviour during the mixing of PG leachate with seawater and the environmental impact due to the enrichment of these pollutants in the particulate phase.

Keywords

Heavy metals, natural radionuclides, phosphogypsum, water mixing, precipitation, acidity.

1. Introduction

Phosphogypsum (PG) is a by-product from the manufacturing fertilizer industry generated during the production of phosphoric acid (H_3PO_4), mainly composed by gypsum ($CaSO_4 \cdot 2H_2O$), but also contains high levels of pollutants such as heavy metals, acids, natural radionuclides, and some others trace elements (Rentería-Villalobos et al., 2010; Madruga et al., 2019) which may be leached. Globally, about 300 Mt of PG are produced every year (Yang et al., 2016) but only 15% of this amount is recycled, being mainly disposed by dumping in large stacks, usually placed in coastal zones close to the factories (Sanders et al., 2013; El Samad et al., 2014). This management of PG frequently generates its weathering by both meteorological and environmental agents which can provoke significant emissions into their surroundings (Tayibi et al., 2009).

Close to the Huelva city (SW of Spain), around 100 Mt of PG are stored in piles on the saltmarshes of the Tinto River estuary covering a surface of about 1000 ha. This PG was generated in five acid phosphoric plants located in the industrial complex of Huelva at a rate of around $2.5 \cdot 10^6$ t/year (Bolívar et al., 2002) since 1965 until the end of 2010, when the production of phosphoric acid stopped. The industrial process is based on the wet chemical attack of phosphate rock ore, in the case of Huelva fluorapatite ($Ca_5(PO_4)_3F$) was used, with sulfuric acid (H_2SO_4). The process can be summarized in the following general reaction (Eq. 1):

$$Ca_5(PO_4)_3F + 5H_2SO_4 + 10H_2O \rightarrow 3H_3PO_4 + 5CaSO_4 \cdot 2H_2O + HF$$

The PG stacks were directly built on the saltmarsh sediments without any type of insulation, and in large proportion of their extension they are currently without any type of cover layer, being exposed to the weathering conditions. Rainfall favors the generation of leachates due to surface runoff and the infiltration provokes the existence of polluted groundwater fluxes. These acidic leachates (pH ≈ 2) show high concentrations of phosphates, sulphates, chlorides,

fluorides, heavy metals (Cd, Cu, Ni, Fe, Mn, Al, Zn, Sb and Sr) (Pérez-López et al., 2016, Millán- Becerro et al., 2019), and U-series radionuclides, being these last ones in the order: $^{238,234}U$ (10^2 Bq L^{-1}), ^{210}Po (10 Bq L^{-1}), and ^{226}Ra and ^{230}Th (1 Bq L^{-1}) (Gázquez et al., 2014; Pérez-Moreno et al., 2018). Previous works (Guerrero et al. 2019, 2020) have demonstrated that the small grain size saltmarsh sediments act as an impermeable barrier for in-depth leachates coming from the PG stacks, and the increase in the concentrations of natural radionuclides and other pollutants only reach the first decimeters of sediments below the contact zone. Therefore, the polluted groundwater travel laterally across the piles to the borders generating small superficial edge outflows in numerous points (Pérez-López et al, 2015, 2016), reaching the estuarine environment. In this regard, the authorities in cooperation with the responsible companies are currently designing an engineering a project for their remediation.

Estuaries are complex coastal systems controlled by tidal action and riverine flows, which comprise transition zones between freshwater and seawater, controlling the flux of elements from the land into the oceans. In these transition systems, meaningful modifications of water chemistry take place with strong gradients in physico-chemical parameters such as pH, redox potential, and dissolved ions (Benoit et al., 1994; Hierro et al., 2014). On the other hand, when anthropogenic polluted releases reach the marine environment, different geochemical processes occur, as precipitation and/or adsorption onto formed solid phases, and on the opposite, dissolution, desorption and migration, changing the elemental concentrations in dissolved phase and the bottom sediments (Zhou et al., 2003; Hierro et al., 2014). Therefore, to study the hydrochemical processes taking place during the mixing of PG leachates with seawater is crucial to understand the intake of radionuclides and other pollutants into the open ocean. One of the main parameters involved in the mixing process is the pH, which directly controls the chemical composition of the mix, and thereby, the precipitation and mineralogy of the particulate phase.

Taking a similar approach to this work, Papaslioti et al. (2018) studied the effects of pH increase on trace elements mobility in the mix of PG leachates with seawater. In regard with the problematic of the leachates, Millán et al. (2019) evaluated the alkaline treatment of this wastewater to provoke the precipitation and immobilization of the dissolved pollutants, achieving the almost totally removal of fluorides, phosphates and most metals with the exception of As and Sb.

According to these facts, the main aim of this work is to evaluate the behaviour of heavy metals and natural radionuclides (U-isotopes and ^{210}Po) and the involved hydrochemical processes during the mixing of phosphogypsum leachates with seawater, simulating the mix produced when the wastewaters from PG piles reach the coast environment.

2. Materials and methods

2.1. Study area

The phosphogypsum stacks of Huelva are over the saltmarshes of the right bank of the Tinto River (Fig. 1). The Tinto River joins in its mouth with the Odiel river to flow into the Atlantic Ocean forming the Huelva Estuary. This estuary is severely polluted (Vicente-Martorell et al., 2009; Cánovas et al. 2010; Sánchez-Moyano et al., 2010) due to both the acid mine drainage (AMD) affecting these two mining rivers which go through the Iberian Pyrite Belt (IPB) transporting in solution high concentrations of metals and metalloids (Sáinz et al. 2004; Nieto et al. 2013), and the intense activity of the Huelva Industrial complex, generating a huge volume of polluted effluents into the estuary.

Figure 1. Location map of the Huelva phosphogypsum stacks and location of the phosphogypsum leachates sampling points: Boreholes (B1 and B2) and perimeter channel (PCh) located in the zone 2 of the phosphogypsum stacks of Huelva.

In their current state, four zones can be identified in the phosphogypsum stacks of Huelva (Fig. 1). Zones 1 and 4 (around 550 ha in total), located to the north and south respectively, are considered already restored. Despite the regeneration of these zones, some edge outflows points can be observed in both, mainly in Zone 4 (Pérez-López et al., 2016). In the Zones 2 and 3, the PG is exposed to the external agents without any kind of cover layer, and show surface ponds of industrial process acidic water (green colors in Fig. 1), which are getting shallower and smaller due to the evaporating process is been developing to proceed with the restoration of this areas. In the Zone 2 about 25 Mt of PG are stored in a surface of over 250 ha forming a pyramidal pile of up to 30 m in height. A network of perimeter channels surrounds this

zone to collect the leachates from the PG stack. The Zone 3, with about 15 Mt of PG piled, shows a surface about 200 ha and an average of 6 m in height.

2.2. Sampling and pretreatment

To develop the mixing experiments, three phosphogypsum leachates (PGL) samples and a seawater sample (SW) of about 200 L were collected on March 2019. The PGL samples, with a volume about 5 L each one, were taken in three different points from the Zone 2, two of them in boreholes (samples B1 and B2) which collect the polluted groundwater in the border of the stack, and the third one inside the perimeter channel (sample PCh), which collects the existing upper lateral leachates. The PGL sampling points were chosen to show similar hydrochemical characteristics than the edge outflows, whose access is complex and a partial mix with the estuarine water is observed. The SW sample was collected in the open ocean close to the Port of Mazagón (Huelva Atlantic coast), to avoid additional contamination due to the high load of metals and other pollutants transported by the Tinto and Odiel rivers due to the AMD as was previously indicated.

The pH, electrical conductivity (EC) and redox potential (Eh) of the samples were measured in situ with a portable multimeter Crison MM40+, with a 5048 (Ag/AgCl) electrode. The instruments were calibrated before sampling, and the redox potential was corrected to obtain the potential relative to the hydrogen electrode (Eh) according to Nordstrom and Wilde (1998). Water samples were filtered in the laboratory by using 0.45 μm pore size polycarbonate filters.

2.3. Titration curves

A titration curve is a plot showing the change of the pH of a solution during a titration, i.e. the addition of a reagent (acid or base). In our case, the objective was to increase the pH of the PGL by the addition of a basic solution. Firstly, a strong base (1.5 M NaOH) was added to the acidic PGL to study its alkaline neutralization improving the knowledge about the kind of leachate acidity. A volume of 100 mL of PGL from the perimeter channel (PCh) was selected, and the reagent was added dropwise with a graduated burette under continuous stirring. The titration curves with SW were carried out to estimate the amount of seawater required to neutralize the leachates to reach pH up to neutral conditions (pH ≈ 7-8). Approximately 300 mL of SW were taken, and each one of the three PGL collected were added individually dropwise with a graduated burette under stirring. For these experiments, the pH values were determined with a multimeter Crison MM40+.

2.4. Precipitation method

The precipitation experiments were developed by using the PGL collected in the perimeter channel (PCh sample), which was selected as the most representative of the leachates arriving to the estuary. For every experiment, 20 mL of PCh

were taken, and the suitable amount of SW (up to around 15 L) to obtain the target pH (3, 4, 5, 6 and 7), according to the obtained ratios in the titration curve. A duplicate of every experiment was carried out, and therefore, ten experiments were developed in total. The mix of SW and PGL was stirred during a few minutes to reach equilibrium (constant pH), and then, it was filtrated through 0.45 μm pore size polycarbonate filters to obtain the precipitates. The physicochemical parameters (pH, Eh and EC, and T) of the resulting solution were measured with a multimeter Crison MM40+. The filtrated solutions (dissolved phase) from each mixing experiment were store and the filters with the formed solid phase were preserved in a dryer until the chemical and radiological analysis were carried out.

2.5. Analytical methodology

Chemical composition of the samples (starting samples and obtained solutions after the experiments) was determined by Coupled Plasma Mass Spectroscopy (ICP-MS) and Inductively coupled plasma optical emission spectroscopy (ICP-OES) techniques at Actlabs (Canada). The quality control (QC) was developed by the measurement of Certified Reference Materials (CRMs) and one duplicate every ten samples.

Natural radionuclides in dissolved and particulate matter were determined by a sequential extraction technique based on the use of tributyl phosphate (TBP) (Bolívar et al., 2000), subsequent electrodeposition onto stainless-steel disc (U-Th-Ra isotopes), and self-deposition onto silver discs for the case of ^{210}Po. The radioactive sources were counted by α-particle spectrometry using ion-implanted silicon detectors, with a 25% absolute efficiency. The QC for alpha-particle measurements was conducted by participating in annual international proficiency tests (International Atomic Energy Agency [IAEA] and the Spanish Nuclear Safety Council [CSN]), and by measuring both a blank and CRMs every set of six samples (IAEA-443).

Two of the obtained precipitates (pH ≈ 5 and 7) were also analyzed by scanning electron microscopy (SEM-EDS), via a JEOL (JSM 5410) scanning electron microscope coupled with a dispersive energy detector in the central research services of the University of Huelva.

3. Results and discussion

3.1. Physicochemical parameters of the starting samples

The physicochemical parameters of the starting samples are shown in Table 1. The SW sample showed typical values of marine waters, with an alkaline pH (≈ 7.8), an electrical conductivity (EC) of 61.5 mS cm^{-1}, due to its high salinity, and a redox potential (Eh) of 465 mV, similar to the observed values for seawaters from Huelva coast and other places worldwide (Papaslioti et al., 2018; Abdel-Halim and Aly-Eldeen.,2016; Akmal Idrus et al., 2017).

Code	pH	EC (mS cm^{-1})	Eh (mV)
SW	7.78	61.5	465
PCh	1.68	40.8	623
B1	1.75	29.4	532
B2	1.62	39.1	414

Table 1. Values of the physicochemical parameters of the starting samples. SW (seawater), PCh (perimeter channel), B1 and 2 (borehole 1 and 2).

Regarding the PGL samples, all of them show extreme acidity (pH ≈ 1.7) as expected, and EC values around 40 mS cm^{-1} for the PCh and B2 samples, while the sample B1 showed a slightly lower value around 30 mS cm^{-1}. The lower EC of the sample B1 is probably related to a higher influence of the rainwater due to sealing problems of the borehole and/or higher weathering of the PG in this point. The Eh of these leachates showed oxidising values in all cases, significantly higher in the sample PCh (Eh ≈ 620 mV) probably due to it is a surface sample, while the samples B1 and B2 are groundwaters from boreholes. As conclusion, to point out that the physicochemical parameters of these leachates are in agreement with the observed ones in previous works (Gázquez et al., 2014; Pérez-Moreno et al., 2018).

3.2. Titration curves

The Figure. 2A displays the titration curve of the sample PCh with a strong base (1.5 M NaOH). The obtained curve shows a similar pattern than the theoretical titration curve with a strong base for the phosphoric acid. Phosphoric acid is a triprotic acid with the following pK_a: pK_{a1} = 2.12, pK_{a2} = 7.21, and pK_{a3} = 12.32 (Haynes et al., 2016), in concordance with the obtained ones in our experimental data. The first two equivalence points, corresponding to base reaction with the first and second protons of this weak acid are also in agreement with the theoretical titration curve. These points were calculated for our experimental data by means of the first and second derivates, being located at pH values 5 and 9, respectively. These facts confirm that the acidity of the leachates comes mainly from the dissolved phosphoric acid in the PGL, which is the main phosphoric acid specie at pH < 2, and not due to other potential acids as fluorhydric acid or not completely consumed sulphuric acid during the industrial chemical process (Eq. 1).

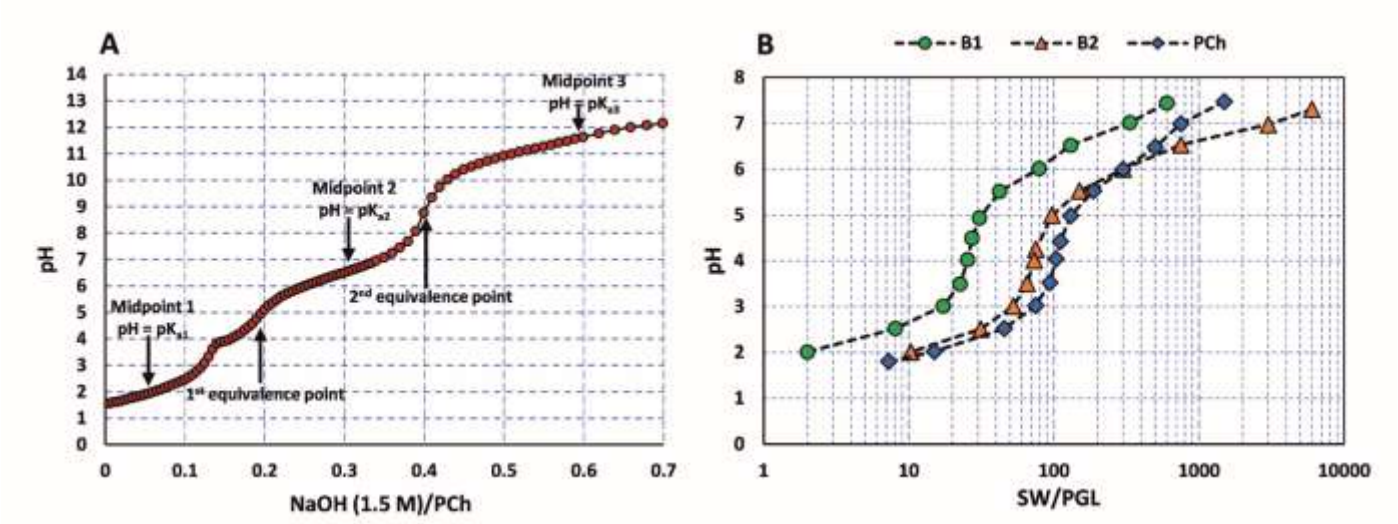

Figure 2. A: Titration curve of the phosphogypsum leachate (PGL) with NaOH (1.5M). B: Titration curves of the phosphogypsum leachates with seawater.

Regarding the curves obtained during the titration of the three collected PGL (B1, B2 and PCh) with SW (Fig. 2B), a similar pattern between them can be observed. Only the first equivalence point, and the first two midpoints (pKa values), are observed. This is because the maximum pH reached by using SW was around 7.5 since the neutralizing power of seawater comes from the presence of carbonates and bicarbonates ions. It is interesting to note the large amount of SW required for the neutralization of the PGL, in the order of 10^3 parts of SW per one part of PGL for reaching a pH = 7. It highlights that the curve for the sample B1 is slightly displaced to the left indicating that a smaller SW amount is required to achieve the alkaline neutralization of this leachate, which is expected, due to the pH of this sample was also slightly higher (Table 1). The curve of sample PCh showed an increase in the slope since SW/PGL = 10^2 in relation to the one of sample B2, which indicates that lower SW amounts are required to increase the pH at this interval. This fact is probably related, despite the similar chemical composition of these two samples as it is discussed in section 3.4, with differences in the concentrations of the dissolved species.

After analyzing these results, it was decided to take the sample collected in the perimeter channel (PCh) to carry out the mixing experiments as was considered the most representative of the leachates that reach the estuary by the edge outflows, and because is the one with the easiest access and the greatest availability in order to carry out future experiments.

3.3. Mixing experiments

The mixing experiments were performed in duplicate (Exp. A and Exp. B), to guarantee the repeatability of the results. The amount of PGL and SW, the physicochemical parameters measured (pH, EC, Eh and T) and the obtained mass of

precipitate for the target pH values are shown in the Table S1 of the supplementary material. The variation of some of these physicochemical parameters during the mixing experiments are displayed in the Figure 3. As can be observed, with equivalent amounts of the starting samples (Fig. 3A) the physicochemical parameters reached very similar values during the neutralization. To confirm this fact, the relative standard deviation (RSD) of the main physicochemical parameters (pH, EC and Eh) was calculated. RSD values < 2 % were obtained with a mean of 0.7 %, verifying the repeatability of the experiment.

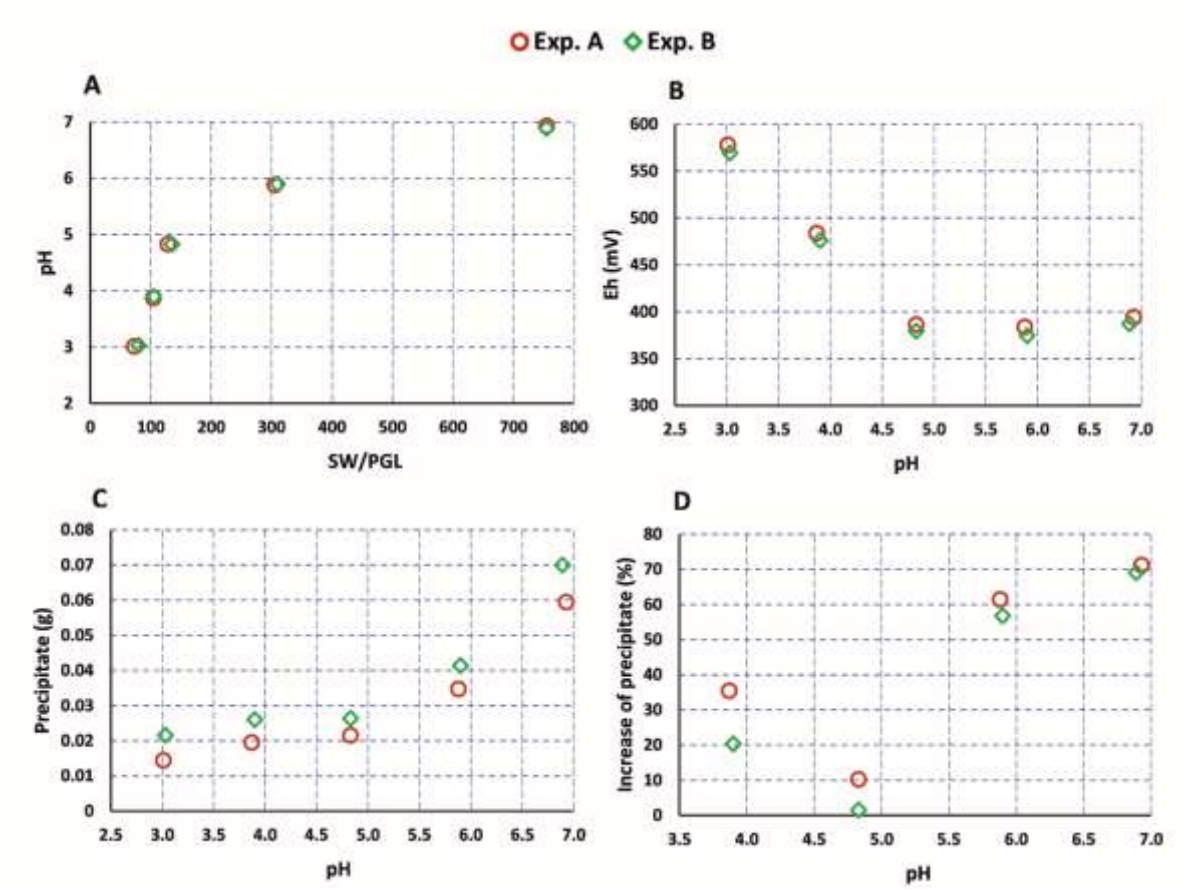

Figure 3. Variation of the pH (A), Eh (B), mass of precipitate (C) and increase of the precipitate (D) during the neutralization carried out in the mixing experiments.

The EC was constant for all the pH range (≈ 64 mS cm^{-1}), showing a similar value than the SW due to the large amounts added in comparison to the PGL ones (see Table S1), which also indicates the scarce precipitation occurred during the neutralization. The Eh decreases during the neutralization from a value close to 600 mV at pH ≈ 3 to around 400 mV at pH ≈ 5, remaining this value constant until pH ≈ 7 (Fig. 3B). This fact seems to be related with the lower influence of the PGL (Eh = 620 mV, Table 1), due to the increase of SW amount at higher pH values, which showed lower Eh value. And, as it was expected, during the mixing experiments, a solid precipitate was generated for each target pH. The obtained masses were very similar in both experiments, being slightly higher for the experiment B (Fig 3C). It highlights

the increase in the mass of precipitates for the pH values 6 and 7 regarding the more acidic pH values. In the Fig. 3D the increase in the mass of the precipitate (%) with respect to the previous pH has also been represented to analyze the precipitate formed per unit of pH increase. It is observed that, from pH ≈ 3 to pH ≈ 4, the mean variation was around 25 %, while the variation was even lower from pH ≈ 4 to pH ≈ 5 with a mean increase of around 5 %. This fact indicates that from pH ≈ 4 to pH ≈ 5 the generated new mass of solid was practically negligible. On the contrary, from pH ≈ 5 to 6, and from pH ≈ 6 to 7 a notable increase in the amount of formed solid was observed, with an average about 65 % in both cases. This fact shows the notable increase in the amount of precipitate generated per unit of pH increase for pH > 5, which indicates that the precipitation of chemical species increases significantly since this pH value.

3.4. Stable elements

In the Table 2 the concentration of the elements in the starting samples, (PGL collected in the PCh and SW), the mixing solutions, and the obtained precipitates for each target pH value in the experiment A are shown. The concentrations of the dissolved elements in the others collected PGL (B1 and B2) are shown in the Table S2 of the supplementary material. Samples PCh and B2 showed similar concentrations in general, while slightly lower concentrations were obtained in B1 in agreement with the lower EC of this sample (Table 1). The concentrations observed in the mixing solutions of the Experiment B were very similar to the ones of the Experiment A as can be consulted in the Table S3 of the supplementary material, and the calculated RSD showed a mean and median values of 6.5 and 2.7 %, respectively. According to the high repeatability observed in this section and section 3.3, the analysis in this work will be performed with the samples of the experiment A.

Regarding the starting samples, the SW contains high concentrations of major elements, such as Na ($11.7 \cdot 10^3$ mg L^{-1}), Mg ($1.44 \cdot 10^3$ mg L^{-1}), S ($1.04 \cdot 10^3$ mg L^{-1}), K and Ca ($4.4 \cdot 10^2$ mg L^{-1}), similar to the found ones in seawater from the Huelva coast in previous studies (Papaslioti et al., 2018; Hierro et al., 2014). The PGL showed high concentrations for major elements, mainly P ($1.1 \cdot 10^4$ mg L^{-1}) being this value 6 orders of magnitude higher than unperturbed freshwater (Wetzel, 2001), but also for most heavy metals, such as Mn, Fe, Zn, As, Cr, Co, Cu, Cd, Ni, Al, Sb and Pb, 2-3 orders of magnitude higher than natural continental waters (Zhou et al., 2020), and U ($1.7 \cdot 10^1$ mg L^{-1}), as expected from the acidic pH value and high EC, and in agreement with previous studies (Pérez-López et al., 2016, Papaslioti et al., 2018). All these pollutants show very low concentrations in the SW, below the detection limit (DL) in most cases, hence its contribution to the concentration of these in the mixing solutions is negligible. In the mixing solutions, the major elements tend to show a constant value during the neutralization, similar to the one of SW, indicating a conservative behaviour, i.e., these elements mainly remain in the aqueous phase. On the other hand, the pollutant elements decrease

their concentrations in the mixing solutions as larger amounts of SW are added, clearly due to the dilution effect, but also precipitation processes can be occurred due to the increase of pH showing a non-conservative behaviour.

	Starting samples		Mixing solutions					Precipitates				
	PGL	SW	pH ≈ 3	pH ≈ 4	pH ≈ 5	pH ≈ 6	pH ≈ 7	pH ≈ 3	pH ≈ 4	pH ≈ 5	pH ≈ 6	pH ≈ 7
Al	6.4	0.13	0.205	0.180	0.170	0.130	0.118	1.0	1.0	1.0	3.5	5.1
Ca	1640	441	457	459	450	443	454	9.3	9.6	14.2	19.3	19.4
Fe	139	0.0081	1.017	0.404	0.271	0.148	0.036	92	97.4	95.4	54.9	39.9
K	268	440	422	432	425	428	438	9.2	9.5	9.2	8.8	9.8
Mg	860	1440	1400	1470	1450	1450	1460	17.1	17.8	18.8	25.5	28.5
Mn	14.3	<0.002	0.190	0.142	0.113	0.036	0.016	0.018	0.027	0.026	0.041	0.050
Co	0.982	<0.002	0.013	0.009	0.007	0.003	<0.002	0.0013	0.0014	0.0012	0.0016	0.0019
Ni	6.82	<0.002	0.081	0.060	0.049	0.021	0.008	0.016	0.014	0.012	0.015	0.016
Na	4620	11700	11540	11900	11800	11900	12050	158	153	137	170	202
P	11281	0.278	139	99	80	34	14	99.7	98.1	99.7	64.8	45.2
S	1523	1040	1031	1070	1050	1053	1060	13.4	11.8	10.3	14.3	18.5
Zn	70	0.050	0.818	0.589	0.483	0.225	0.118	0.16	0.16	0.76	1.97	1.81
Cr	20	<0.002	0.165	0.049	0.006	<0.002	<0.002	17.1	20.2	16.3	13.7	5.3
Si	519	<2	7.5	5.3	4.4	<2	<2	0.60	0.41	0.43	0.26	0.15
Cu	9.84	0.0035	0.121	0.092	0.068	0.022	0.006	0.16	0.08	0.31	0.99	1.02
As	21.6	<0.002	0.387	0.287	0.229	0.099	0.040	0.127	0.161	0.172	0.108	0.083
Sr	34.3	8.2	8.5	8.5	8.4	8.2	8.3	0.24	0.45	0.83	1.02	0.85
Cd	9.5	<0.002	0.115	0.082	0.067	0.028	0.010	0.0033	0.0022	0.0036	0.0047	0.0029
Ba	0.042	0.008	0.008	0.008	0.007	0.007	0.007	0.034	0.034	0.067	0.071	0.064
Sb	0.567	0.011	0.036	0.030	0.022	0.017	0.016	0.0066	0.0185	0.0144	0.0113	0.0065
Pb	0.55	0.003	0.010	0.006	0.004	0.003	0.003	0.068	0.21	0.42	0.37	0.24
U	19.1	0.0032	0.30	0.11	0.008	0.013	0.024	2.1	12.4	18.4	10.0	2.0

Table 2. Concentration (mg L^{-1}) of the most significant elements in the starting samples and in the mixing solutions, and solid precipitates (mg g^{-1}) in the experiment A.

The obtained precipitates are mainly composed by Na, and Fe (Table 2). High concentration of most heavy metals and U was observed in these precipitates with values about 1-3 orders of magnitude higher than the background of this region (Lario et., 2016; Guerrero et al., 2019), which demonstrate the high polluting potential of the leachates into the PG stacks surroundings and the urgency of restoration measures. The concentrations of these pollutants in the solid phase during the neutralization process showed different trends, increasing, decreasing, or not showing a clear behaviour. To clarify these results and to analyze the non-conservative character of these elements, the transfer factor (TF) to solid was calculated according to the following formula (Eq. 2):

$$\frac{C_p \cdot M_p}{C_{PGL} \cdot V_{PGL} + C_{SW} \cdot V_{SW}} \cdot 100$$

Where:

C_p = Concentration of the element in the precipitate

M_p = Mass of the precipitate

C_{PGL} = Concentration of the element in the PGL

V_{PGL} = Volume of PGL

C_{SW} = Concentration of the element in the SW

V_{SW} = Volume of SW

To note that the TF to aqueous phase was also calculated and the data are in agreement with the obtained ones to solid, but were presented these last ones due to the authors consider it more accuracy as a direct measure. For the elements with concentrations below the DL in the SW, this value was applied for the calculations. TF values < 0.1 % of Ca, K, Mg, Na, S, Si, Sr and Cd and < 1 % of Mn, Co, Ni, As, Sb and P were obtained, showing a conservative behaviour of the major elements and some heavy metals during the neutralization. To note that, the TF only indicate the % of an element that is transferred into the solid phase, hence should be taken into account the total amount of this element added to the mixing solutions, which explain the fact that P and Na are some of the main components of the precipitate due their very high concentration in the starting samples.

The other elements, including several heavy metals, showed higher TF to solid (Fig. 4), and therefore a non-conservative behaviour during the neutralization, precipitating and/or been adsorbed to a greater or lesser extent onto the solid phase.

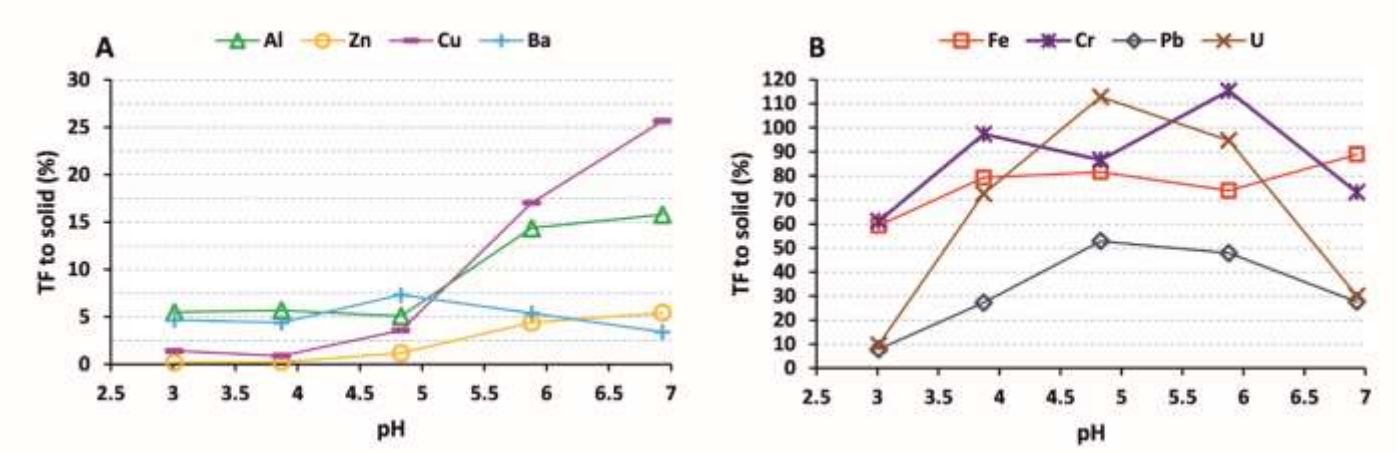

Figure 4. Transfer factor (TF) to solid (%) of non-conservative elements.

Zn and Cu showed a conservative behaviour until pH ≈ 5, increasing theirs TF up to 5 and 25 % at pH ≈ 7, respectively (Fig. 4A). Ba showed TF around 5 % during the neutralization while Al increases its TF since pH ≈ 6 – 7 reaching values about 15 % (Fig. 4A). On the other hand, Fe, Pb, Cr and U showed a notably higher TF to solid (Fig. 4B). Regarding Pb, the maximum TF (≈ 50 %) was observed at pH values around 5 – 6, while the TF to solid of Fe ranged from around 60 % at pH ≈ 3 to 90 % at pH ≈ 7. A mean TF around 90 % of Cr was observed during the neutralization. According to Papaslioti et al. (2018), Fe tends to precipitate in the form of phosphates as strengite ($FePO_4 \cdot 2H_2O$) at pH

> 3 and in the form of oxyhydroxide as goethite (α-FeOOH) at pH > 4, lepidocrocite (γ-FeOOH) nearly at pH > 5 and ferrihydrite [$Fe(OH)_3$] at pH > 6, which usually act as sinks for trace elements as Pb and Cr, being retained by sorption processes. Lastly, the TF of U increased from a minimum about 10 % at pH ≈ 3 to reach a total precipitation at pH ≈ 5 and decreased again up to 30 % at pH ≈ 7. This behaviour will be discussed in detail in the next section.

3.5. Natural radionuclides

The activity concentration of ^{238}U and ^{210}Po and the $^{234}U/^{238}U$ activity ratio in the starting samples, the mixing solutions, and the obtained precipitates for each target pH in the experiment A are shown in the Table 3. Ra and Th-isotopes showed low activity concentrations in the PGL with values below 2 Bq L^{-1}, being in the mixing solutions below the DL (1 mBq L^{-1}) in most cases, hence were not included in this work. The PGL showed, due to their high acidity, very high activity concentrations for the studied natural radionuclides, with about 300 Bq L^{-1} of ^{238}U and 22 Bq L^{-1} of ^{210}Po. These values are about 4 – 5 orders of magnitude higher than the observed ones in unperturbed surface freshwater and seawater (De Vos and Tarvainen, 2006; IAEA, 2017), which demonstrates the extreme polluting potential of these acidic leachates. Although U concentrations in seawater depends on the salinity (Owens et al., 2011), its concentration is significantly uniform in the world oceans, being generally accepted that the U "oceanic average" concentration is 3.3 ± 0.2 mg L^{-1}, i.e., 0.041 Bq L^{-1} of ^{238}U (Ku et al., 1977), in agreement with our experimental data. The $^{234}U/^{238}U$ activity ratio (AR_U) showed secular equilibrium in the PGL ($AR_U = 1$), same ratio than the measured in both PG and phosphate rock used in Huelva and other places worldwide (Boryło et al., 2009; El Afifi et al., 2009, Guerrero et al., 2020) due to the uniform bulk dissolution of the original ore in the phosphoric acid production process (Hussain and Krishnaswami,1980; Andersen et al., 2009). In the SW sample the AR_U was a bit higher (1.08 ± 0.04), in agreement with mean value of marine water ($AR_U = 1.14$) (Boryło and Skwarzec, 2014). In surface waters this ratio is usually higher than 1 due to nuclide recoil during alpha-decay of ^{238}U and preferential dissolution of ^{234}U (Henderson et al., 2006).

		^{238}U	$^{234}U/^{238}U$	^{210}Po
Starting samples	PGL	302 ± 9	1.00 ± 0.01	21.8 ± 1.0
	SW	0.042 ± 0.002	1.08 ± 0.04	0.0036 ± 0.0004
Mixing solutions	pH ≈ 3	3.56 ± 0.17	0.99 ± 0.01	0.19 ± 0.02
	pH ≈ 4	1.473 ± 0.029	1.00 ± 0.02	0.075 ± 0.010
	pH ≈ 5	0.177 ± 0.009	1.02 ± 0.03	0.021 ± 0.005
	pH ≈ 6	0.219 ± 0.018	1.03 ± 0.03	0.006 ± 0.001
	pH ≈ 7	0.325 ± 0.017	1.02 ± 0.02	0.0037 ± 0.0010

	pH ≈ 3	22.4 ± 0.6	0.99 ± 0.01	7.6 ± 0.2
	pH ≈ 4	124 ± 2	1.00 ± 0.02	10.6 ± 0.2
Precipitates	pH ≈ 5	232 ± 12	1.006 ± 0.006	17.0 ± 0.3
	pH ≈ 6	115 ± 5	1.005 ± 0.006	11.8 ± 0.4
	pH ≈ 7	20.7 ± 0.9	1.01 ± 0.01	7.7 ± 0.3

Table 3. Activity concentration (Bq L^{-1}) of the studied radionuclides in the starting samples and the mixing solutions, and in the solid precipitates (Bq g^{-1}).

The activity concentrations of natural radionuclides in the mixing solutions showed a clear decrease during the neutralization, due to the dilution effect by the large amount of SW added, similarly as was previously observed for the stable elements. To note that the activity concentration of ^{210}Po in the solutions continuous decreasing with the increase of pH, while the ^{238}U reach the minimum concentration at pH ≈ 5 and tends to increase again at higher pH values. It highlights that ^{210}Po showed a similar value than SW at pH ≈ 7, while ^{238}U showed activity concentrations 1- 2 orders of magnitude higher than the SW concentration in the mixing solutions. Concerning the solid precipitates, ^{238}U and ^{210}Po showed a similar trend, being enriched the precipitate until pH ≈ 5 and decreasing again their concentrations as the pH value increase. The measured concentrations of these natural radionuclides in the precipitates are 2-3 orders of magnitude higher than the worldwide median value for natural soils (0.035 Bq g^{-1}) (UNSCEAR 2000), showing once again the potential environmental impact of these leachates. The AR_U showed values around secular equilibrium in both mixing solutions and precipitates, demonstrating that is strongly influenced by the PGL.

To clarify the behaviour of U-isotopes and ^{210}Po during the alkaline neutralization of the acidic leachates, the TF to solid and the distribution coefficients (K_d) were calculated (Fig. 5). The K_d are used to quantify the affinity of a chemical specie for particles and were calculated according to the following formula (Eq. 3):

$$K_d = \frac{C_p}{C_d}$$

Where:

C_p = activity concentration of the radionuclide in the precipitate

C_d = activity concentration of the radionuclide in the dissolution

The TF to solid of ^{238}U increased gradually their value from about 10 % at pH ≈ 3, up to about 90 % at pH ≈ 5, when most of the ^{238}U is found in the precipitate (Fig. 5A). The TF slightly decreased at pH ≈ 6 to about a 70 %, but reached a 20 % at pH ≈ 7, which indicates that at this pH about 80 % of ^{238}U is again in solution. This fact is confirmed in the Fig. 5B where the K_d at pH ≈ 5 – 6 are around 1-2 orders of magnitude higher than for lower or higher pH values. This

behaviour has been observed in previous studies (Hsi and Langmuir, 1985; Serkiz and Johnson, 1994) and was justify due to coprecipitation of U with Fe-Mn hydroxides (McKee et al., 1987) in the pH range from 4 to 6 and the existence of redissolution processes due to the formation of carbonated complexes (Hierro et al., 2013; Guerrero et al., 2021) at higher pH values. Therefore, the U-isotopes show a non-conservative behaviour and tend to precipitate or to be adsorbed almost totally at pH values around 5, to return into the liquid phase due to redissolution/desorption processes at near neutral pH values.

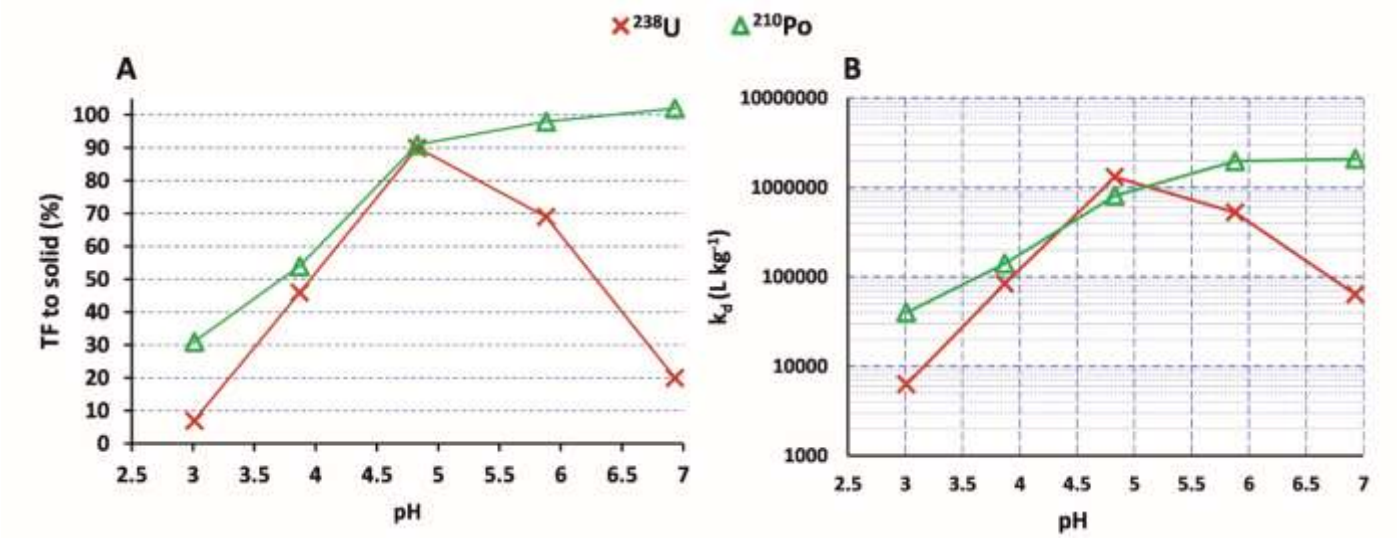

Figure 5. Transfer factor (TF) to solid (%) (A) and evolution of the distribution coefficients (kd) during the increase of pH (B) of the studied radionuclides

The ^{210}Po continuously increased its TF during the alkaline neutralization of the PGL, reaching values around 90 % at pH values ≈ 5, and a total removal (TF ≈ 100 %) at pH value ≈ 7 (Fig. 5B). In this sense, the K_d values of ^{210}Po increase during the increase of pH, showing values around one order of magnitude higher for pH values above 4, than for lower pH values. The observed K_d are in agreement with the obtained ones in other works in natural (unperturbed) and polluted systems worldwide (Blasco et al., 2016, Manjón et al., 2019, Bam et al., 2020). These facts demonstrate that ^{210}Po tends to precipitate and/or to be adsorbed by the particulate matter during the neutralization, showing a non-conservative behaviour.

3.6. Micro-structural characterization of the obtained precipitates

According to the previous findings, several heavy metals and the studied natural radionuclides showed a non-conservative behaviour during the increase of pH, been removed from the dissolved into the solid phase. Thus, the characterization of the obtained precipitates is of great significance to improve the understanding of the geochemical processes controlling its mobility during the neutralization of the PGL with SW. The precipitates generated from two

target pH were analyzed by SEM-EDS, and the images and spectra are shown in the Figure 6A (pH ≈ 5) and B (pH ≈ 7). The results of this analysis showed that the formed precipitates consist of a cryptocrystalline matrix mainly composed of P and Fe, as expected according to results presented in section 3.4, suggesting precipitation of iron phosphates, as strengite ($FePO_4 \cdot 2H_2O$). A fine layer of salts mainly composed by Cl and Na, probably in the form of halite (NaCl), covering most of the matrix particles was observed (Fig. 6A). These salts were probably originated by the evaporation of the remaining solution (mostly SW) in the filter.

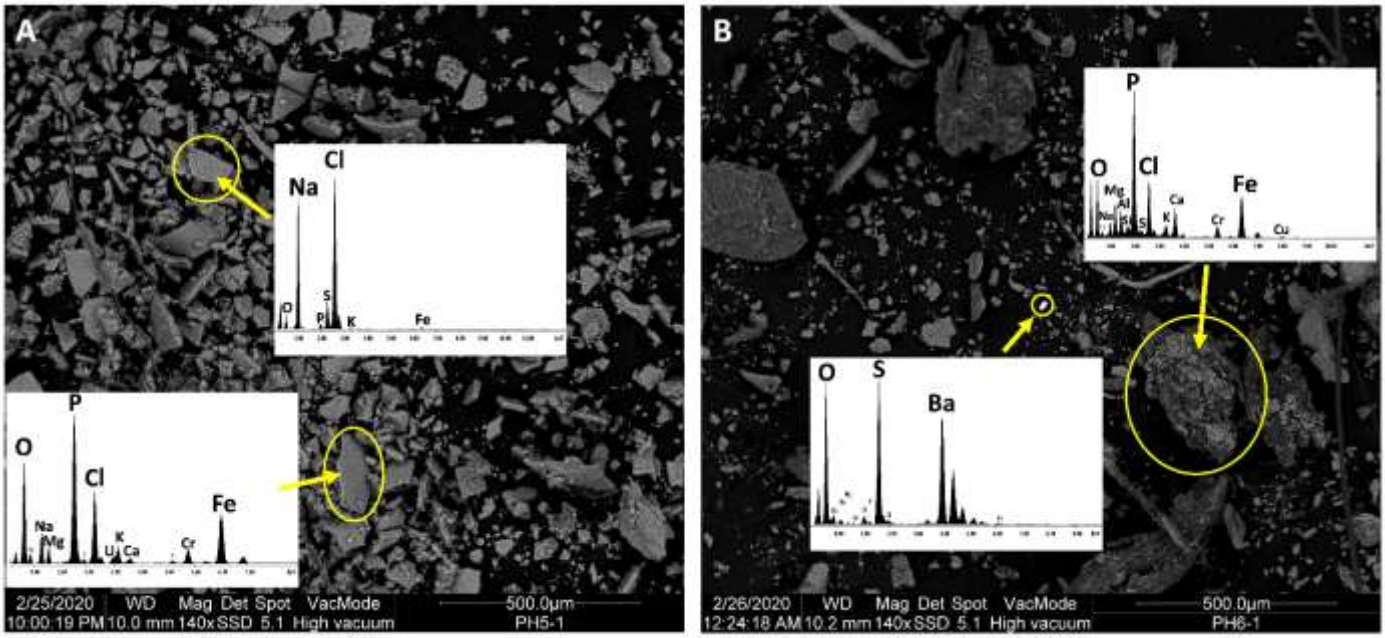

Figure 6. SEM images and EDS spectra of the obtained precipitates during the neutralization at pH ≈ 5 (A) and 7 (B).

It is very interesting the detection of U in the matrix at pH ≈ 5 (Fig. 6A), which is in agreement with the previous findings and seems to confirm that U is removed from the dissolved phase due to coprecipitation/adsorption processes onto strengite crystals. Other metals, such as Al, Cr and Cu were detected together with the matrix at pH ≈ 7 (Fig. 6B), which is consistent with the observed data in section 3.4, and probably due to coprecipitation and/or adsorption processes. The higher concentrations of Ca detected at pH ≈ 7 in the matrix together with the high concentration of P could be indicative of the precipitation of hydroxyapatite [$Ca_5(PO_4)_3(OH)$]. Finally, to highlight the small particle mainly composed by S and Ba, probably as barium sulphate in the form of barite ($BaSO_4$), observed at pH ≈ 7. Barite show a very low solubility and tend to precipitate when the concentration of sulphate increases in solution, in this case due to the input from the PGL.

4. Conclusions

The PG stacks of Huelva release polluted acidic leachates into the surrounding estuarine environment which produce a serious environmental impact. Seawater mixing experiments were carried out to improve the understanding of the

hydrochemical processes occurring when these leachates reach the marine environment increasing their pH, focusing on the behaviour of heavy metals and the natural radionuclides with higher concentrations in the leachates (U-isotopes and ^{210}Po).

The obtained conclusions in this work are:

1. The titration curve of the phosphogypsum leachate with a strong base (NaOH) confirmed that the acidity of the leachates is mainly due to the existence of remaining phosphoric acid, and not due to other potential acids as fluorhydric acid coming from the ore, or sulphuric acid not completely consumed during the industrial chemical process.
2. The acidic phosphogypsum leachates show a high pollutant load, with large amounts of heavy metals as Mn, Fe, Zn, As, Cr, Co, Cu, Cd, Ni, Al, Sb and Pb, 2-3 orders of magnitude higher than natural continental waters, and natural radionuclides, mainly U-isotopes and ^{210}Po, 4 - 5 orders of magnitude higher than unperturbed surface freshwater and seawater. This fact demonstrates the extreme polluting potential of these acidic leachates.
3. The analysis of the transfer factor (TF) to solid showed a conservative behaviour during the alkaline neutralization of major elements and some heavy metals as Ni, Cd, As, Sb and Co, which remain almost totally in the aqueous phase. Several heavy metals as Al, Fe, Cr, Zn, Cu, Ba, and Pb showed higher TF to solid, and therefore a non-conservative behaviour during the neutralization, precipitating and/or been adsorbed to a greater or lesser extent onto the solid phase.
4. The U-isotopes and ^{210}Po showed a clear non-conservative behaviour according to the TF and distribution coefficient (K_d) values. U-isotopes presented an almost total removal from the dissolved phase at pH values around 5, probably due to coprecipitation/adsorption processes onto the formed precipitates, to return into the liquid phase due to redissolution/desorption processes at near neutral pH values. ^{210}Po strongly increases its removal from the dissolved phase during the neutralization, reaching a total removal at pH $\approx$ 7 due to precipitation and or coprecipitation/adsorption onto solid precipitates.
5. The formed precipitates during the neutralization showed heavy metal and natural radionuclide (U-isotopes and ^{210}Po) concentrations from 1 to 3 orders of magnitude higher than unperturbed soils, demonstrating the serious environmental impact produced by the stacks into their surroundings in their current state.

The SEM-EDS images showed that the generated precipitates consist of a cryptocrystalline matrix mainly composed of P and Fe, due to the precipitation of iron phosphates (strengite), which act as a sink for heavy metals and natural radionuclides by coprecipitation/adsorption processes.

5. Funding

This work was partially supported by Spanish Ministry of Economy and Competitiveness [project number, CTM2015-68628-R], the Spanish Ministry of Science, Innovation and Universities [project number, EQC2018-004306-P], the Regional Government of Andalusia [project number, FEDER2018-UHU-1255876] and the Spanish Ministry of Education [grant number FPU15/00646].

6. References

Abdel-Halim, A. M., and Aly-Eldeen, M. A., 2016. Characteristics of Mediterranean Sea water in vicinity of Sidikerir Region, west of Alexandria, Egypt. The Egyptian Journal of Aquatic Research, 42(2), 133–140. DOI: 10.1016/j.ejar.2016.05.002

Akmal Idrus, F., Dennis Chong, M., Syazwani Abd Rahim, N., Mohd basri, M., Musel, J., 2017. Physicochemical Parameters ofSurface Seawater in MalaysiaExclusiveEconomic Zones Off the Coast of Sarawak. Borneo Journal of Resource Science and Technology 7(1):1-10. DOI: 10.33736/bjrst.388.2017

Andersen, M.B., Erel, Y., Bourdon, B., 2009. Experimental evidence for 234U-238U fractionation during granite weathering with implications for 234U/238U in natural waters. Geochim. Cosmochim. Acta 73, 4124-4141. DOI: 10.1016/j.gca.2009.04.020

Bam, W., Maiti, K., Baskaran, M., Krupp, K., Lam, P. J., & Xiang, Y., 2020. Variability in 210Pb and 210Po partition coefficients (Kd) along the US GEOTRACES Arctic transect. Marine Chemistry, 103749. DOI:10.1016/j.marchem.2020.103749

Benoit, G., Oktay-Marshall, S.D., Cantu, A., Hood, E.M., Coleman, C.H., Corapcioglu, M.O, Santschi, P.H., 1994. Partitioning of Cu, Pb, Ag, Zn, Fe, Al, and Mn between filter-retained particles, colloids, and solution in six Texas estuaries. Mar. Chem. 45, 307–36. DOI:10.1016/0304-4203(94)90076-0

Blasco, M., Gázquez, M. J., Pérez-Moreno, S. M., Grande, J. A., Valente, T., Santisteban, M., de la Torre, M.I., Bolívar, J. P., 2016. Polonium behaviour in reservoirs potentially affected by acid mine drainage (AMD) in the Iberian Pyrite Belt (SW of Spain). Journal of Environmental Radioactivity, 152, 60–69. DOI:10.1016/j.jenvrad.2015.11.008

Bolívar, J.P., García-Tenorio, R., Vaca, F., 2000. Radioecological study of an estuarine system located in the south of Spain. Water Research, 34(11), 2941–2950. DOI: 10.1016/s0043-1354(99)00370-x

Bolívar, J.P., García-Tenorio, R., Más, J.L., Vaca, F., 2002. Radioactive impact in sediments from an estuarine system affected by industrial waste releases. Environ. Int. 27, 639e645. DOI:10.1016/S0160-4120(01)00123-4.

Boryło, A., and Skwarzec, B., 2014. Activity disequilibrium between 234U and 238U isotopes in natural environment. J. Radioanal. Nucl. Ch., 300(2), 719–727. DOI :10.1007/s10967-014-3001-9

De Vos, W., Tarvainen, T., 2006. The Geochemical Atlas of Europe Part 2. Interpretation of Geochemical Maps, Additional Tables, Figures, Maps, and Related Publications. 690 pp.

Cánovas, C. R., Olías, M., Nieto, J. M., and Galván, L., 2010. Wash-out processes of evaporitic sulfate salts in the Tinto River: Hydrogeochemical evolution and environmental impact. Appl. Geochem., 25(2), 288–301. DOI:10.1016/j.apgeochem.2009.11.014

El Afifi, E.M., Hilal, M.A., Attallah, M.F., EL-Reefy, S.A., 2009. Characterization of phosphogypsum wastes associated with phosphoric acid and fertilizers production. J. Environ. Radioact. 100 (5), 407-412. DOI:10.1016/ j.jenvrad.2009.01.005.

El Samad, O., Aoun, M., Nsouli, B., Khalaf, G., Hamze M., 2014. Investigation of the radiological impact on the coastal environment surrounding a fertilizer plant. J. Environ. Radioact., 133, pp. 69-74. DOI:10.1016/j.jenvrad.2013.05.009

Gázquez, M. J., Mantero, J., Mosqueda, F., Bolívar, J. P., García-Tenorio, R., 2014. Radioactive characterization of leachates and efflorescences in the neighbouring areas of a phosphogypsum disposal site as a preliminary step before its restoration. J. Environ. Radioact, 137, 79–87. DOI:10.1016/j.jenvrad.2014.06.025.

Guerrero, J. L., Gutiérrez-Álvarez, I., Mosqueda, F., Olías, M., García-Tenorio, R., & Bolívar, J. P., 2019. Pollution evaluation on the salt-marshes under the phosphogypsum stacks of Huelva due to deep leachates. Chemosphere, 230, 219–229. DOI:10.1016/j.chemosphere.2019.04.212

Guerrero, J. L., Gutiérrez-Álvarez, I., Mosqueda, F., Gázquez, M. J., García-Tenorio, R., Olías, M., Bolívar, J. P., 2020. Evaluation of the radioactive pollution in the salt-marshes under a phosphogypsum stack system. Environmental Pollution, 113729. DOI: 10.1016/j.envpol.2019.113729

Guerrero, J.L., Gutiérrez-Álvarez, I., Hierro, A., Pérez-Moreno, S.M., Olías, M., Bolívar, J.P., 2021. Seasonal evolution of natural radionuclides in two rivers affected by acid mine drainage and phosphogypsum pollution. Catena, 104978. https://doi.org/10.1016/j.catena.2020.104978.

Hsi, D., Langmuir, D., 1985. Adsorption of uranyl onto ferric oxyhydroxides: Application of the surface complexation site-binding model. Geochim. Cosmochim. AC., 49(9), 1931–1941. DOI:10.1016/0016-7037(85)90088-2

Henderson, G. M., Hall, B. L., Smith, A., Robinson, L. F., 2006. Control on (234U/238U) in lake water: A study in the Dry Valleys of Antarctica. Chem. Geol., 226(3-4), 298–308. DOI: 10.1016/j.chemgeo.2005.09.026

Hierro, A., Martín, J.E., Olías, M., Vaca, F., Bolívar, J.P., 2013. Uranium behaviour in an estuary polluted by mining and industrial effluents: the Ría of Huelva (SW of Spain). Water Res. 47, 6269–6279. DOI: 10.1016/j.watres.2013.07.044

456 Hierro, A., Olías, M., Ketterer, M.E., Vaca, F., Borrego, J., Cánovas, C.R., Bolívar, J.P., 2014. Geochemical behavior
457 of metals and metalloids in an estuary affected by acid mine drainage (AMD). Environ Sci Pollut Res 21, 2611–2627.
458 DOI:10.1007/s11356-013-2189-5
459 Hussain, N., Krishnaswami, S., 1980. U-238 series radioactive disequilibrium in groundwaters: implications to the
460 origin of excess U-234 and fate of reactive pollutants. Geochim. Cosmochim. Acta 44 (9), 1287-1291. DOI:
461 10.1016/0016-7037(80)90089-7
462 IAEA, 2017. The Environmental behaviour of Polonium. Technical Reports Ser. Nº 484.
463 Ku, T. L., Knauss, K. G., Mathieu, G. G., 1977. Uranium in open ocean: concentration and isotopic composition. Deep
464 Sea Research, 24(11), 1005–1017. doi:10.1016/0146-6291(77)90571-9
465 Millán-Becerro, R., Pérez-López, R., Macías, F., Cánovas, C., Papaslioti, EM., Basallote, MD., 2019. Assessment of
466 metals mobility during the alkaline treatment of highly acid phosphogypsum leachates. Sci. Total, Environ. 660, 395-
467 405. DOI:10.1016/j.scitotenv.2018.12.305
468 Lario, J., Alonso-Azcárate, J., Spencer, C., Zazo, C., Goy, J. L., Cabero, A., … García-Ródriguez, M., 2016. Evolution
469 of the pollution in the Piedras River Natural Site (Gulf of Cadiz, southern Spain) during the Holocene. Environmental
470 Earth Sciences, 75(6). DOI:10.1007/s12665-016-5344-8
471 McKee, B. A., DeMaster, D. J., Nittrouer, C. A., 1987. Uranium geochemistry on the Amazon shelf: Evidence for
472 uranium release from bottom sediments. Geochim. Cosmochim. AC., 51(10), 2779–2786. DOI:10.1016/0016-
473 7037(87)90157-8
474 Madruga, M.J., Prudencio, M.I., Gil Corisco J.A. Mihalik, J., Marques, R., Santos, M., Reis, M., Paiva, I., Dias, M.I.,
475 2019. Int J Waste Resour, 9:1. DOI: 10.35248/2252-5211.19.9.363
476 Manjón, G., Mantero, J., Vioque, I., Díaz-Francés, I., Galván, J. A., Chakiri, S., Choukri, A., García-Tenorio, R., 2019.
477 Natural radionuclides (NORM) in a Moroccan river affected by former conventional metal mining activities. Journal of
478 Sustainable Mining, 18(1), 45–51. DOI:10.1016/j.jsm.2019.02.003
479 Millán-Becerro, R., Pérez-López, R., Macías, F., Cánovas, C. R., Papaslioti, E.-M., & Dolores Basallote, M., 2019.
480 Assessment of metals mobility during the alkaline treatment of highly acid phosphogypsum leachates. Science of The
481 Total Environment, 660, 395–405. DOI: 10.1016/j.scitotenv.2018.12.305
482 Nieto, J.M., Sarmiento, A.M., Canovas, C.R., Olias, M., Ayora, C., 2013. Acid mine drainage in the Iberian Pyrite Belt:
483 1. Hydrochemical characteristics and pollutant load of the Tinto and Odiel rivers. Environ. Sci. Pollut. Res. Int. 20 (11),
484 7509–7519. DOI:10.1007/s11356-013-1634-9

485 Nordstrom, D.K., Wilde, F.D., 1998. Reduction-oxidation potential (electrode method). In: National Field Manual for
486 the Collection of Water Quality Data. US Geological Survey Techniques of Water-resources Investigations. Book 9,
487 Chap. 6.5.
488 Owens, S.A., Buesseler, K.O., Sims, K.W.W., 2011. Re-evaluating the 238U-salinity relationship in seawater:
489 Implications for the 238U-234Th disequilibrium method. Marine Chemistry 127, 31-39. DOI:
490 10.1016/j.marchem.2011.07.005
491 Papaslioti, E.M., Pérez-López, R., Parviainen, A., Sarmiento, A.M., Nieto, J.M., Marchesi, C., Garrido, C.J., 2018.
492 Effects of seawater mixing on the mobility of trace elements in acid phosphogypsum leachates. Mar. Pollut. Bull. 127,
493 695–703. DOI: 10.1016/j.marpolbul.2018.01.001.
494 Pérez-López, R., Nieto, J.M., de la Rosa, J.D., Bolívar, J.P., 2015. Environmental tracers for elucidating the weathering
495 process in a phosphogypsum disposal site: implications for restoration. J. Hydrol. 529, 1313–1323. DOI:10.1016/j.
496 jhydrol.2015.08.056.
497 Pérez-López, R., Macías, F., Cánovas, C.R., Sarmiento, A.M., Pérez-Moreno, S.M., 2016. Pollutant flows from a
498 phosphogypsum disposal area to an estuarine environment: an insight from geochemical signatures. Sci. Total Environ.
499 553, 42–51. DOI: 10.1016/j.scitotenv.2016.02.070
500 Pérez-Moreno, S.M., Gázquez, M.J., Pérez-López, R., Vioque, J., Bolívar, J.P., 2018. Assessment of natural
501 radionuclides mobility in a phosphogypsum disposal area. Chemosphere 211, 775-783. DOI:
502 10.1016/j.chemosphere.2018.07.193
503 Rentería-Villalobos, M., Vioque, I., Mantero, J., Manjón, G., 2010. Radiological, chemical and morphological
504 characterizations of phosphate rock and phosphogypsum from phosphoric acid factories in SW Spain. J. Hazard Mater.
505 181, 193-203. DOI:10.1016/j.jhazmat.2010.04.116
506 Sáinz ,A., Grande, J.A, de la Torre, M.L., 2004. Characterisation of heavy metal discharge into the Ria of Huelva.
507 Environ Int 2004;30:557–66. DOI: 10.1016/j.envint.2003.10.013
508 Sanders, L.M., Luiz-Silva, W., Machado, W., Sanders, C.J., Marotta, H., Enrich-Prast, A., Bosco-Santos, A., Boden,
509 A., Silva, E.V., Santos, I.R., Patchineelam S.R., 2013. Rare earth element and radionuclide distribution in surface
510 sediments along an estuarine system affected by fertilizer industry contamination. Water Air Soil Pollut 224, 1742. DOI:
511 10.1007/s11270-013-1742-7

Sánchez-Moyano, J. E., García-Asencio, I., and García-Gómez, J. C., 2010. Spatial and temporal variation of the benthic macrofauna in a grossly polluted estuary from southwestern Spain. Helgol. Mar. Res., 64(3), 155–168. DOI:10.1007/s10152-009-0175-6

Serkiz, S.M., Johnson, W.H., 1994. Uranium Geochemistry in Soil and Groundwater at the F and H Seepage Basins (U). EPD-SGS-94-307. Westinghouse Savannah River Company, Savannah River Site, Aiken, South Carolina. DOI: 10.2172/10194263

Tayibi, H., Choura, M., L opez, F.A., Alguacil, F.J., L opez-Delgado, A., 2009. Environmental impact and management of phosphogypsum. J. Environ. Manag. 90 (8), 2377-2386. DOI: 10.1016/j.jenvman.2009.03.007.

UNSCEAR, 2000. Sources and Effects of Ionizing Radiation. Volume I: Sources: Report to the General Assembly of the United Nations Scientific Committee on the Effects of Atomic Radiation. United Nations, New York.

Vicente-Martorell, J. J., Galindo-Riaño, M. D., García-Vargas, M., and Granado-Castro, M. D., 2009. Bioavailability of heavy metals monitoring water, sediments and fish species from a polluted estuary. J.Hazard. Mater., 162(2-3), 823–836. DOI:10.1016/j.jhazmat.2008.05.1061157-016-9398-6

Wetzel, R.G., 2001. Limnology. Academic Press, New York, 1006 pp.

Yang, L., Zhang, Y., Yan, Y., 2016. Utilization of original phosphogypsum as raw material for the preparation of self-leveling mortar. J. Clean. Prod. 127, 204e213. DOI: 10.1016/j.jclepro.2016.04.054.

Zhou, J., Liu, Y., Abrahams, P., 2003. Trace metal behaviour in the Conwy estuary, NorthWales. Chemosphere 51 (5), 429–440. DOI:10.1016/S0045-6535(02)00853-6

Zhou, Q., Yang, N., Li, Y., Ren, B., Ding, X., Bian, H., & Yao, X. (2020). Total concentrations and sources of heavy metal pollution in global river and lake water bodies from 1972 to 2017. Global Ecology and Conservation, e00925. DOI: 10.1016/j.gecco.2020.e00925